

# Mechanical Fracture Behavior of Polyacetal and Thermoplastic Polyurethane Elastomer Toughened Polyacetal

FENG-CHIH CHANG\* and MI-YUN YANG

*Institute of Applied Chemistry  
National Chiao-tung University  
Hsinchu, Taiwan, Republic of China*

Polyacetal (POM) toughening with thermoplastic polyurethane (TPU) elastomer was investigated in terms of rheological, mechanical, and morphological properties. Polyacetal can be effectively toughened by the blending with TPU elastomer and the improvement on toughness is found most significant with TPU content from 20 to 30 percent. POM does fracture in ductile mode under extremely low deformation rate and the ductile-brittle transition rate is at 0.5 mm/min. The transition rate is increased with the increase of elastomer content. The precrack hysteresis energy is important in dictating the failure mode. The experimental results show the hysteresis energy (under constant load) increases with the increase of elastomer content and the decrease of deformation rate. Greater hysteresis energy results in larger precrack plastic zone size and thus tends to shift the fracture mode from brittle to ductile as the critical size of the plastic zone is reached. The adoption of the slow rate fracture method has the advantages of ranking toughness of very brittle polymeric materials *vs.* the conventional Izod or Charpy impact method by varying temperatures. FTIR shows significant interaction between POM and TPU which is probably responsible for the TPU elastomer being such an efficient toughening agent for POM. Delamination in the buffer zone between the plane-strain and the plane-stress is discovered and the possible mechanism is discussed.

## INTRODUCTION

From the time that formaldehyde was first isolated by Butlerov (1) in 1859, polymeric forms have been encountered by those handling the material. Nevertheless it is since the late 1950's only that polymers have been available with the requisite stability and toughness to make them useful plastics. In the early 1940's an intensive research program on the polymerization of formaldehyde was initiated by the Du Pont Company and eventually came out with commercial products as Delrin (2, 3). Celanese later developed an alternative approach to produce the thermally stable polyoxymethylenes (POM) and marketed as Celcon (4). Like many unmodified polymer matrices, polyacetal is extremely brittle in notched impact. Cherdon, *et al.* (5) disclosed improving the impact strength of polyacetal compositions by blending with various copolymers. Wurmb, *et al.* (6) disclosed improving the physical properties (including impact strength) of glass fiber reinforced POM compositions by blending with high MW thermoplastic polyurethane. Pritchard (7) disclosed improving im-

pact resistance of POM by blending a rubbery polymeric material having a  $T_g$  below 0°C and preferable as particles of less than 20 microns. Burg (8) also disclosed the improvement of POM impact resistance by adding a mixture of an elastomeric and a hard polymer. Bronstert (9) disclosed the toughening of POM with an elastomeric graft copolymer having  $T_g$  below -20°C. Burg (10) later disclosed the POM compositions that contain a third component of a segmented thermoplastic copolyester or a polyurethane. Flexman (11-13) disclosed a series POM/TPU compositions indicating extraordinary impact resistance. Flexman (14) later compared the impact resistance of the toughened polyacetal and the based resin and suggested some aspects of its fracture mechanism. Chiang, *et al.* (15) reported the mechanical properties of polyacetal/polyurethane blends. Almost all the available literature (except two—14 and 15) in rubber toughening polyacetal are patents and the fundamental information in this major engineering thermoplastic is rather scarce. Polyacetal is one of the four major engineering thermoplastics because of its metal-like high strength and high stiffness. Polyacetal also possesses high creep, fatigue, and corrosive

\* To whom correspondence should be addressed.

resistance that leads to numerous commercial applications such as bearings, gears, conveyor belts, blower wheels, cams, fan blades, pump impellers, and carburetor bodies. This paper describes polyacetal toughening with thermoplastic polyurethane elastomer in terms of rheological, mechanical, and morphological properties.

## MATERIALS AND EXPERIMENTAL PROCEDURES

The polyacetal Celcon M 90 used in this study is produced commercially by Hoechst Celanese. The thermoplastic polyurethane elastomer Elastollan R S90A50 was obtained from Elastogran of West Germany. The TPU elastomer was mixed with polyacetal in the appropriate ratios using a 30 mm single screw extruder ( $L/D = 30$ ) with compression ratio 3/1 and in the temperature range 165 to 180°C. Tensile and flexural (Izod) specimens were prepared by an Arburg model 270-210-500 injection molding machine with  $L/D = 20$  and temperature range 180 to 200°C. A capillary rheometer (a Rheograph 2001 from Gottfert company) was used to measure the viscosity as function of shear rate. Tensile (ASTM D 638) and flexural (ASTM D 790) properties were carried out by an Instron universal testing machine model 4201. Notched Izod impact tests varying notch radius and temperature were carried out in a TMI impacter equipped with a temperature-controlled chamber which can be operated from -100 to 150°C. The method to determine impact critical strain energy release rate by varying depth of notch was previously developed (16) and adopted in this study using 0.127 mm notch radius and at ambient conditions. In order to investigate the effect of deformation rate and hysteresis energy in a notched fracture, combination of an Instron and an Izod setup were employed as shown in Fig. 1. Scanning electron microscopy of the fractured surfaces was carried out on a Hitachi S-570 SEM. The samples were typically sputter-coated with an Au/Pd alloy. FTIR analysis using ATR technique on a Bomem model DA3.002 FTIR was employed. Dynamic viscoelastic properties, storage modulus ( $E'$ ), loss modulus ( $E''$ ), and  $\tan\delta$  were measured in a Rheovibron DDV II dynamic viscoelastometer at a heating rate of 1 to 2°C/min and frequency of 11 Hz in the temperature range from -120 to 120°C.

## RESULTS AND DISCUSSION

### Rheological Properties

The viscosity vs. shear rate behavior of POM, POM/TPU blends, and TPU at 185°C (results from 198 and 210°C are not shown here) is illustrated in Fig. 2. For the pure matrix, TPU has higher activation energy,  $E$ , for the flow process according to the Andrade or Arrhenius equation,

$$\eta = K \exp(E/RT)$$

TPU has higher viscosity than POM at 185°C and the

order is reversed at around 190°C where all the blends and matrices have almost identical viscosity. Curve E of Fig. 3 clearly shows almost the same viscosity from all the blends at 185°C and shear rate of 3,000  $s^{-1}$  independent of TPU contents. The flow behavior of mixtures of two immiscible uncross-linked polymers can be very complex and unpredictable. Wu (17) studied the droplet size in the viscoelastic polymer system and found the critical Weber number,  $G\eta_m a_n/\gamma$ , is function of viscosity ratio. The Weber number (and thus the dispersed droplet size) is at minimum when the viscosity ratio is near one. The processing temperature of about 190°C employed in the present study should be the ideal viscosity ratio for the formation of the smallest droplets.

### Tensile Properties

The stress strain curves of tensile testing of POM and POM containing various amounts of TPU elastomer are shown in Fig. 4. The composition containing 30 percent TPU shows dramatic increase in elongation to break while the modulus and yielding strength are decreased with the increase of TPU content as

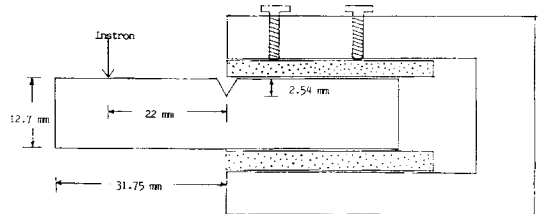


Fig. 1. The clamp device for slow rate deformation fracture and hysteresis cyclic studies.

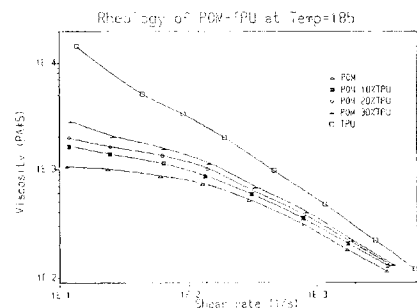


Fig. 2. Plots of viscosity vs. shear rate at 185°C.

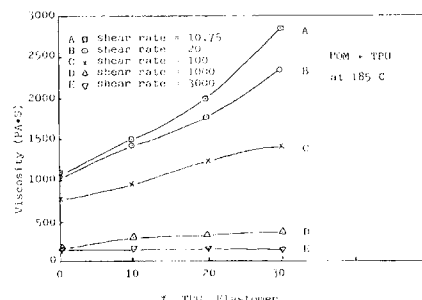


Fig. 3. Effect of elastomer content on viscosity at various shear rates.

would be expected. Figures 5A–D are the photomicrographs of the surfaces from the cryogenically fractured tensile specimens (after tensile testing to break) at the plane parallel to elongation. It is clearly shown that the extensively elongated specimen, POM + 30 percent TPU (180 percent strain), has a large amount of matrix drawing and voids. Table 1 summarizes both tensile and flexural properties.

Izod Impact Properties

Figure 6 and Table 2 demonstrate the effect of TPU content and temperature on Izod impact strength in a standard 3.175 mm thickness specimen with 0.254 mm notched radius. The temperature shows very little effect on the pure POM matrix with impact energy of 0.15 to 0.25 J (47 to 79 J/m) which is fairly close to the results previously reported (14). The presence of TPU elastomer significantly in-

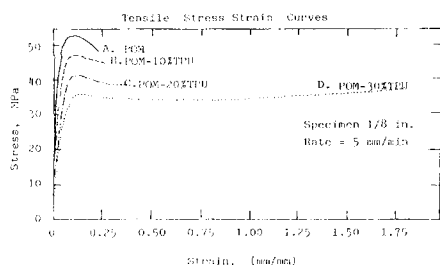


Fig. 4. Tensile stress strain curves for POM and TPU elastomer toughened POM.

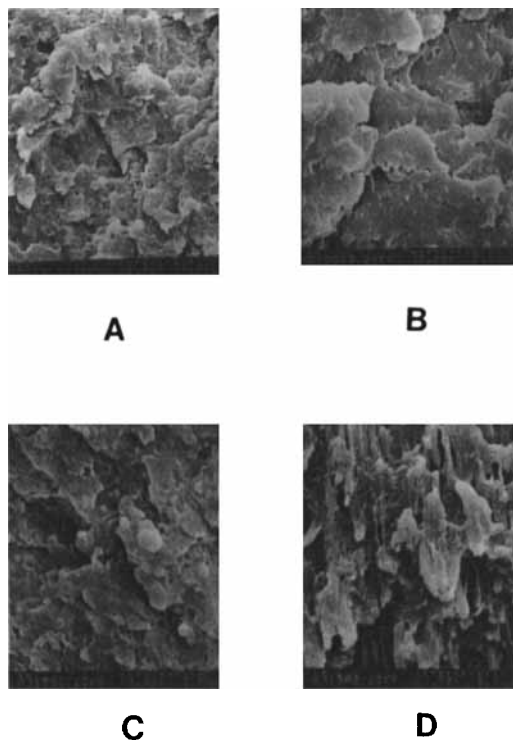


Fig. 5. SEM photomicrographs of the tensile specimens elongated to break at the plane parallel to elongation direction, A: POM, B: POM + 10 percent TPU, C: POM + 20 percent TPU, D: POM + 30 percent TPU.

Table 1. Tensile and Flexural Properties.

Sample	Tensile Test			Flexural Test	
	Stress at Yield (Mpa)	Modulus (Mpa)	Elongation %	Stress at Yield (Mpa)	Modulus (Mpa)
POM	52.1	2818.6	55.0	69.7	2580.3
10U	47.1	2057.4	64.5	61.3	2374.8
20U	41.2	1778.9	85.0	50.6	1783.6
30U	35.8	1288.4	409.6	41.5	1496.5

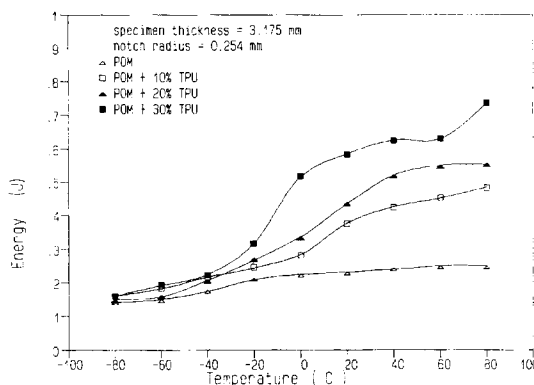


Fig. 6. Izod impact energy of 1/8 in. specimens vs. testing temperature.

Table 2. Izod Impact Energy at Various Temperatures.\*

Temperature (°C)	Impact Energy**			
	POM J	POM + 10% TPU J	POM + 20% TPU J	POM + 30% TPU J
-80	0.140	0.160	0.150	0.160
-60	0.150	0.182	0.158	0.192
-40	0.175	0.218	0.208	0.226
-20	0.210	0.245	0.268	0.318
0	0.225	0.285	0.338	0.515
20	0.232	0.378	0.435	0.585
40	0.240	0.425	0.520	0.625
60	0.250	0.452	0.550	0.630
80	0.250	0.485	0.552	0.735

\* Notch radius: 0.254 mm; specimen thickness: 3.175 mm.  
 \*\* To convert impact unit J/M, multiple a factor of 314.96.

creases the impact strength of POM as the temperatures are above -20°C. Figure 7 shows the effect of the notch radius on impact strength indicating notch sensitivity of POM and the TPU toughened POM. The POM + 30 percent TPU blend shows almost linear relationship between notch radius and Izod impact strength. Under Izod impact rate of about 3 m/s, essentially all compositions fractured brittle without lateral constriction (characteristics of ductile fracture) being observed on the fractured surfaces.

Notch Fracture under Slow Strain Rates

Time-temperature equivalence of polymeric materials has received extensive investigations through creep or stress-relaxation but relatively little work has been reported on fracture behavior. The conventional Charpy and the Izod methods have been employed as basic impact tests with constant impact

velocity and a single impact energy value. Although the value of the composite energy obtained from the notched Charpy or Izod measurement without knowing details during fracture process is arguable, these methods indeed have the advantages of being easily performed to provide information for ranking materials in order of impact toughness over a range of test temperatures. For most notch brittle polymers such as POM, PET, PBT, SAN, and PS, strict relying on changes in testing temperatures to determine the material ductile brittle transition to rank their toughness is almost impossible. By applying the general principle of time-temperature relation, reduce impact velocity approach is a viable method to replace the commonly employed temperature to study polymer fracture behavior. The advantages are numerous including the popularity of Instron instrument and detailed information are obtained such as load-displacement relation during fracture. *Figure 8* demonstrates a typical example for the plots of load-displacements of POM and TPU toughened POM under a cross-head rate of 1.0 mm/min which is much slower in comparing with 180 m/min from a typical Izod impact test. POM and POM + 10 percent TPU are brittle fracture with only initiation energy while POM + 20 percent TPU and POM + 30 percent TPU are ductile failure with clear initiation and propagation energies. *Figure 9* demonstrates the ductile brittle transition phenomenon by varying deformation velocities. The transition velocity of POM is at about 0.5 mm/min and progressively increases with the increase of TPU content. This result demonstrates that even the commonly believed very notch brittle material such as POM can actually fracture ductile under very slow deformation velocity and how the elastomer toughens the brittle matrix. Similar observations were extended to other highly notch brittle polymeric materials such as PET and PBT and will be reported in the future. The composition, POM + 30 percent TPU, has the ductile-brittle transition velocity at approximately 0.2 m/min at ambient temperature which is still far below the regular Izod impact velocity (180 m/min). Therefore the results from previous Izod tests are essentially all in brittle fracture. The impact energies of POM + 30 percent

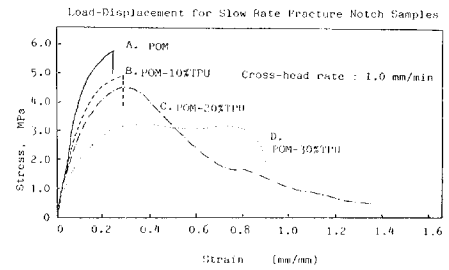


Fig. 8. Load-displacement relation of slow deformation to fracture at 1.0 mm/min deformation rate for POM and TPU toughened POM.

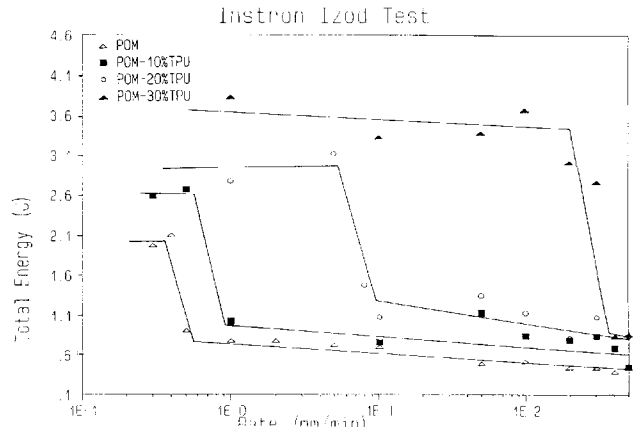


Fig. 9. Ductile-brittle transition rates of POM and TPU elastomer toughened POM.

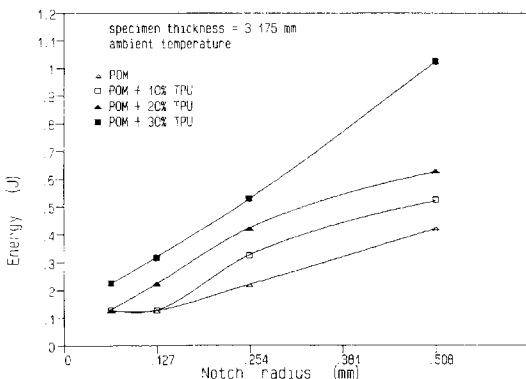


Fig. 7. Izod impact energy of 1/8 in. Specimens vs. notch radius at ambient conditions.

TPU are 3.3 J (977 J/m) for ductile failure and 0.8 J (252 J/m) for brittle failure compared with 0.58 J (183 J/m) for brittle failure from the high speed Izod test. Other interesting observations worthy to mention are the higher fracture energy resulting from the TPU elastomer contained POM than the POM matrix itself both in ductile and brittle fracture which is very similar to other crystalline polymer such as nylon. However, the elastomer modified amorphous polycarbonate actually has less fracture energy than the polycarbonate matrix when fractures in ductile mode but higher fracture energy when fractures in brittle mode (18). The photographs of the resultant specimens after fracture tests under various deformation rates are shown in *Figs. 10A-C* where the ductile to brittle transition rates of various compositions can be visually identified. The SEM photographs of POM fractured surfaces in ductile and brittle failure due to the change in deformation rates in two magnifications ( $\times 20$  and  $\times 1000$ ) are shown in *Figs. 11A-D*. At high magnification, the brittle fractured surface (*Fig. 11B*) shows typically the brittle fracture with flake-like structure. The ductile fractured surface (*Fig. 11D*) shows lots of fiber-like drawings which is totally different from the ductile fractured surface from polycarbonate (18). *Figure 11C* clearly shows the presence of mass shear yield with lateral constriction on both sides of the specimen. The distance of the lateral constriction is measured at 0.185 mm on each side which is about 11.6 percent

of the total thickness (3.17 mm). No sign of lateral constriction can be found from the brittle fractured surface (Fig. 11A). Very similar results were obtained from the POM/TPU = 90/10 blend (Figs. 12A-D) except more yield on the surface and slight increase in the length of the lateral constriction (0.223 mm). Figures 13 and 14 show the higher elastomer containing compositions that have even higher drawing extent on those fiber-like textures (Figs. 13D and 14D) of the ductile fractured surfaces and the distances of lateral constriction are also increased. Slightly lateral constriction is noticed near the root of the notch in the brittle fractured surfaces of the TPU toughened POM (Figs. 13A and 14A). The crack initiates through the relatively smaller precrack plastic zone and a competition of ductile and brittle modes of

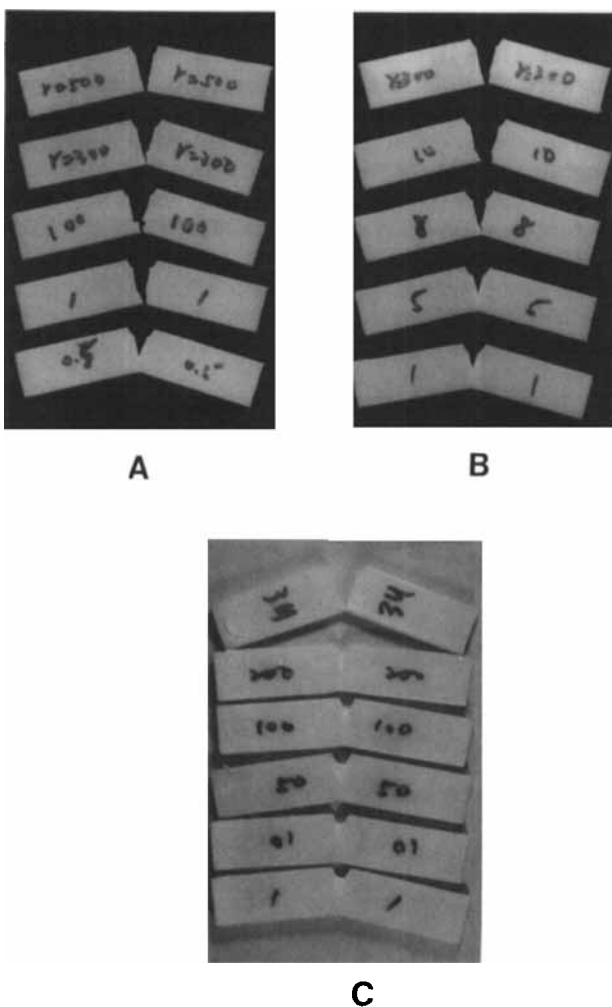


Fig. 10. Sideview photographs of the ductile and brittle fractured specimens under various deformation rates.

- A: POM + 10 percent TPU  
a:  $\dot{r} = 500$  mm/min, b:  $\dot{r} = 300$  mm/min, c:  $\dot{r} = 100$  mm/min, d:  $\dot{r} = 1$  mm/min, e:  $\dot{r} = 0.5$  mm/min.
- B: POM + 20 percent TPU  
a:  $\dot{r} = 300$  mm/min, b:  $\dot{r} = 10$  mm/min, c:  $\dot{r} = 8$  mm/min, d:  $\dot{r} = 5$  mm/min, e:  $\dot{r} = 1$  mm/min.
- C: POM + 30 percent TPU  
a:  $\dot{r} = 500$  mm/min, b:  $\dot{r} = 200$  mm/min, c:  $\dot{r} = 100$  mm/min, d:  $\dot{r} = 50$  mm/min, e:  $\dot{r} = 10$  mm/min, f:  $\dot{r} = 1$  mm/min.

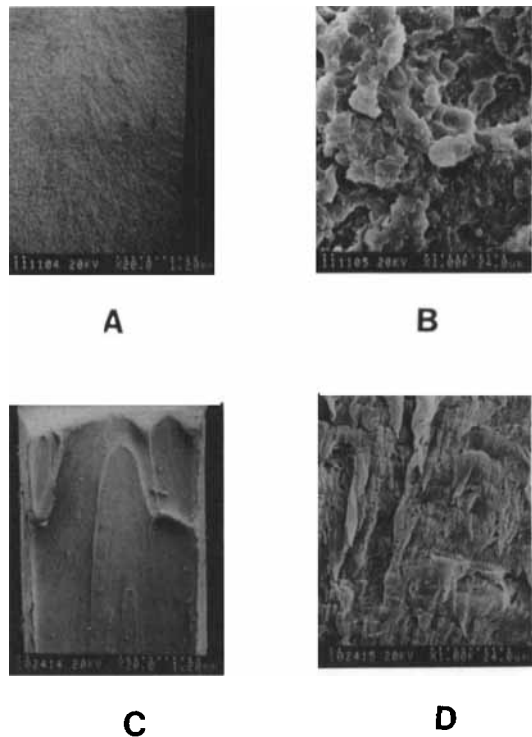


Fig. 11. Two magnification SEM photographs for POM in ductile and brittle fractured surfaces.

- A: Rate = 100 mm/min, brittle,  $\times 20$
- B: Rate = 100 mm/min, brittle,  $\times 1000$
- C: Rate = 0.5 mm/min, ductile,  $\times 20$
- D: Rate = 0.5 mm/min, ductile,  $\times 1000$ .

fracture takes place during the early stage of crack propagation. Due to high deformation rate, the critical size of the plastic zone (to be explained later) is not quite established, the propagating crack front will quickly pass through the relatively smaller plastic zone and results in brittle fracture. Delamination occurs in the boundary between the plane-stress and plane-strain region (Figs. 13C and 14C) because of the complicated triaxial stress field. According to a von Mises yielding criterion, the shape of plastic zone radius at crack tip is smaller in the central plane strain region than edge plane stress region by a factor of at least three. Therefore the strain gradient of the unyielded material immediately outside the yielding zone increases sharply in the buffer boundary between the plane strain and plane stress region. The stress for yielding in this buffer zone is less than in plane strain conditions ( $6\gamma + 6\alpha$ ) but still higher than in the plane stress conditions ( $6\gamma$ ). The higher stress resulted from the higher strain in this buffer zone exceeds the stress required for cavitation or craze formation before reaching the stress for yielding and thus initiates the delamination process. The delaminated buffer zone shown in Figs. 13C and 14C consists of a band of highly drawn texture that indicates shear stress resultant from the complex triaxial stress may evolve during the delamination process. This slow fracture, identical to the regular Izod impact method except for velocity, can be employed to rank polymer toughness easier than the Izod method

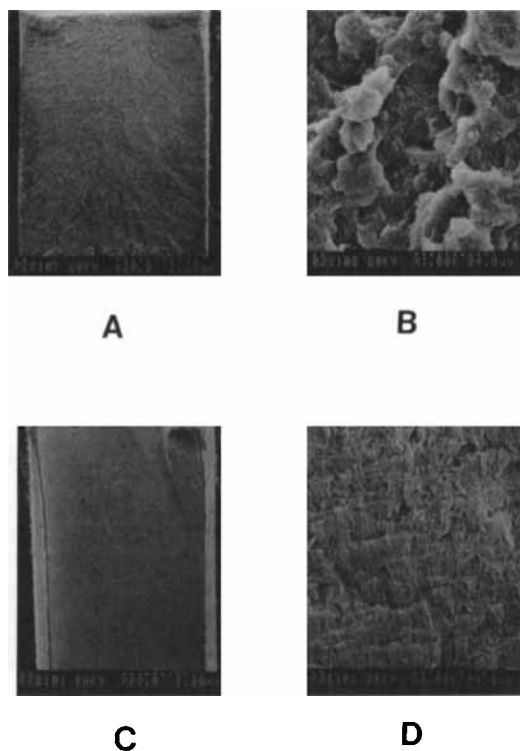


Fig. 12. Two magnification SEM photographs for POM + 10 percent TPU elastomer in ductile and brittle fractured surfaces.

A: Rate = 300 mm/min, brittle,  $\times 20$

B: Rate = 300 mm/min, brittle,  $\times 1000$

C: Rate = 0.5 mm/min, ductile,  $\times 20$

D: Rate = 0.5 mm/min, ductile,  $\times 1000$ .

by varying the temperature, and more information concerning the fracture behavior can be obtained.

#### Pre-crack Hysteresis (Loss) Energy

Linear fracture mechanics is based on the assumptions of linear elasticity and infinitesimal strain which is certainly not true especially in the highly strained vicinity of the crack tip when the plastic zone is formed. Andrews (19–22) proposed a generalized theory of fracture mechanics which is able to lift the serious constraints imposed by the requirements of the classical fracture mechanics. Andrews emphasized that the stored strain energy available for crack initiation is the input energy minus the hysteresis (loss) energy. Such viscoelastic and plastic energy losses have been largely neglected because they are considered insignificant and close to the crack tip in a typical brittle fracture. However, the loss energy becomes significant and important in some semi-ductile polymers or brittle polymers under very slow deformation velocity or high temperature. Figure 15 shows curves of a complete deformation to fracture and several hysteresis cycles (data came from different specimens) at various load values of POM at 0.3 mm/min deformation rate. Similar hysteresis curves from the TPU elastomer toughened POM at constant cross-head rate of 2.0 mm/min are present in Fig. 16. Complete data of hysteresis study

are summarized in Table 3. Results from Figs. 15 and 16 all point out that higher load levels result in higher percentage of hysteresis ratio, deformation strain, and energy. The TPU modified POM has higher hysteresis ratio than POM itself at same load levels. The hysteresis energy and hysteresis ratio of POM at constant load (20 Kg) but varying deformation rates are shown in Fig. 17. The hysteresis ratio of POM increases from 21.43 percent at rate of 100 mm/min to 48.86 percent at rate of 0.3 mm/min. In a notched beam test, the strain rate at the notch tip is considerably higher and has been estimated to be the order of  $5 \times 10^3 \text{ s}^{-1}$  (23). The Eyring theory gives the relationship between strain rate ( $\dot{\epsilon}$ ) and yield stress ( $\sigma_y$ ) and the plot of  $\sigma_y/T$  vs.  $\log \dot{\epsilon}$  should give a set of parallel lines for different temperatures. Therefore, higher strain rate results in higher yield stress near the crack tip and relatively smaller plastic zone size with less hysteresis energy at same load can be expected. Figure 18 summarizes the relation of hysteresis ratio and deformation rate at two different load levels for POM and 10 percent TPU elastomer toughened POM. At the same load and rate, the elastomer containing POM is about 10 percent higher in hysteresis ratio than the matrix POM. The pre-crack hysteresis loops can occur due to viscoelasticity, plasticity, and crazes or microvoids for less ductile polymeric materials. These three or four types of pre-crack energy dissipation processes do not occur separately

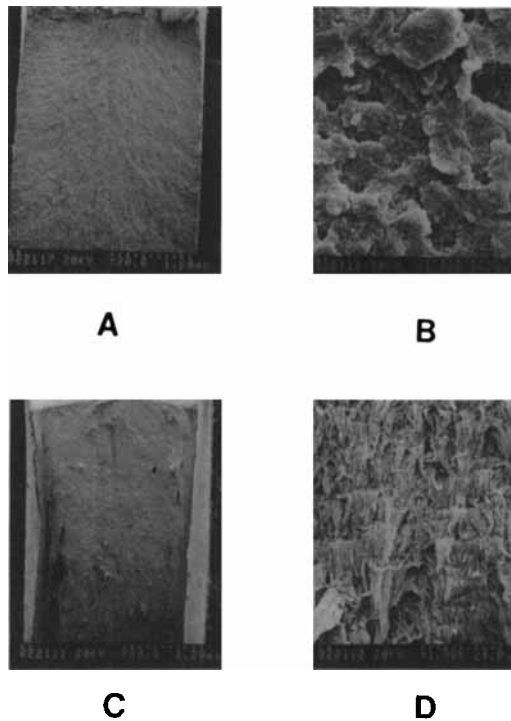


Fig. 13. Two magnification SEM photographs for POM + 20 percent TPU elastomer in ductile and brittle fractured surfaces.

A: Rate = 100 mm/min, brittle,  $\times 20$

B: Rate = 100 mm/min, brittle,  $\times 1000$

C: Rate = 1.0 mm/min, ductile,  $\times 20$

D: Rate = 1.0 mm/min, ductile,  $\times 1000$ .

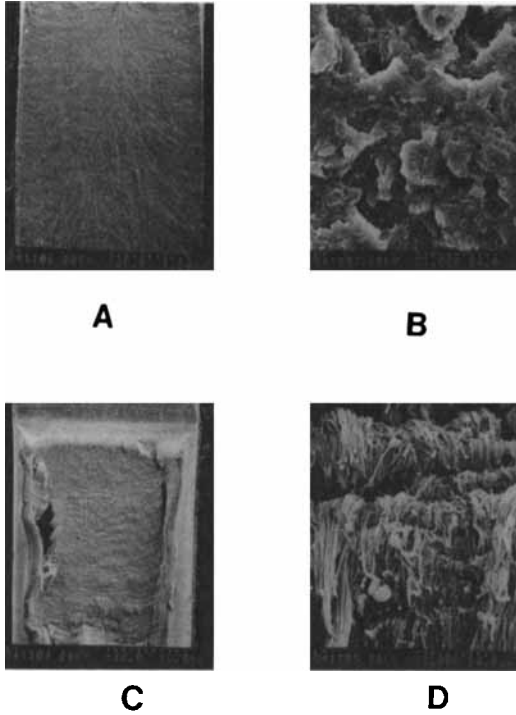


Fig. 14. Two magnification SEM photographs for POM + 30 percent TPU elastomer in ductile and brittle fractured surfaces.

- A: Rate = 500 mm/min, brittle,  $\times 20$
- B: Rate = 500 mm/min, brittle,  $\times 1000$
- C: Rate = 20 mm/min, ductile,  $\times 20$
- D: Rate = 20 mm/min, ductile,  $\times 1000$ .

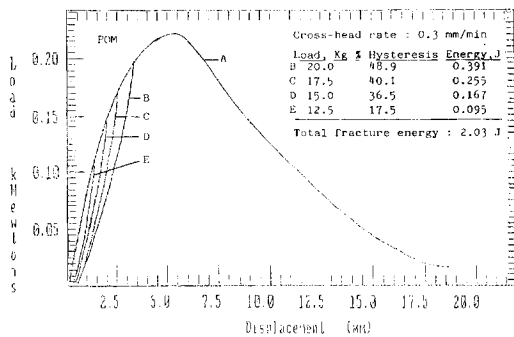


Fig. 15. Load-displacement relation for POM deforming to break and hysteresis cycle at deformation rate of 0.3 mm/min.

but are superimposed on each other. Distinction between or quantifying these complicated and overlapping processes in any deformation is difficult or almost impossible experimentally. However, the trend of higher hysteresis energy resulting in higher pre-crack plasticity is undeniable. The higher hysteresis energy is expected to reduce the stored elastic energy available for crack initiation and create greater plastic zone volume ahead of the crack tip. When a crack propagates through and within this precrack plastic zone, ductile tearing occurs. To assure a complete ductile fracture, the new plastic zone in front of the propagating crack tip is formed immediately and al-

ways stays ahead of the propagating crack front. If the precrack plastic zone is too small at the moment of crack initiation, the momentum carried by the crack front can easily propagate and pass through the precrack plastic zone; a brittle failure occurs. One form of semi-ductile failure occurs when the propagating crack front catches up with the plastic zone during the fracture process. How large a pre-crack plastic zone and how quick the new plastic zone must be formed following the crack initiation in order to contain the propagating crack front are determined by the materials and many experimental parameters such as deformation rate, geometry, notch radius, temperature, and specimen thickness. The higher deformation strain (which relates to the load) results in greater hysteresis energy and thus has a larger precrack plastic volume. A critical plastic volume is assumed to exist for the brittle to ductile transition and the most important factor to increase the plastic zone is the crack initiation strain. Brown (24) pointed out that the notch impact strength of thermoplastics is a measure of difficulty of initiating the moving crack. Therefore any effort to toughen the thermoplastics is to delay the crack initiation, and the presence of soft rubber in a hard matrix indeed serves this purpose.

**Dynamic Mechanical Properties**

The storage modulus,  $E'$ , loss modulus,  $E''$ , and loss tangent,  $\tan\delta$  of POM and POM + 30 percent TPU are plotted against temperature in Fig. 19. The dynamic measurements were carried out at a frequency of 11 Hz and temperatures from  $-120$  to  $120^\circ\text{C}$ . At temperature below  $-100^\circ\text{C}$ , the storage modulus of POM + 30 percent TPU is lower than POM matrix when both components of the blend are in glassy stage. With increasing temperature, the amplitude of vibrational motions becomes roughly comparable to the potential energy barriers of segmental motions. The peak maximum temperature of  $\tan\delta$  at  $-64^\circ\text{C}$  (Fig. 19, curve A<sub>3</sub>) corresponds to the  $T_g$  of the POM which is slightly higher than  $T_g$  previously reported at  $-73^\circ\text{C}$  (15) probably due to different material sources. Two peaks at  $-64$  and  $-57^\circ\text{C}$  are present in the  $\tan$  curve of POM + 30 percent TPU corresponding to  $T_g$ s of POM and TPU. No shift of POM  $T_g$  in the

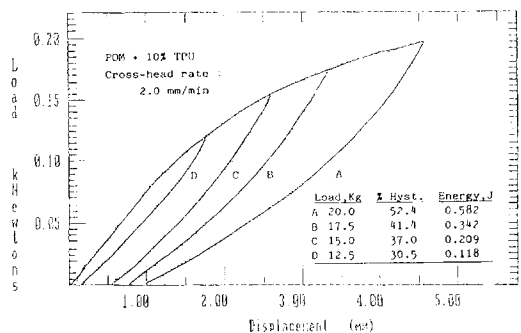


Fig. 16. Load-displacement relation of hysteresis cycles for POM + 10 percent TPU elastomer at deformation rate of 2.0 mm/min.

Table 3. Hysteresis Properties of POM and POM + 10 Percent TPU.

			Load kg			
			20	17.5	15	12.5
A. POM	0.3 mm/min	%Hyst.	48.8	40.0	36.5	17.3
		Energy, J	0.39	0.26	0.17	0.10
		Disp. mm	3.40	2.52	2.00	1.40
	2.0 mm/min	%Hyst.	43.7	26.3	23.9	16.8
		Energy, J	0.34	0.23	0.15	0.09
		Disp. mm	2.95	2.25	1.86	1.32
	20 mm/min	%Hyst.	31.1	20.6	14.4	12.0
		Energy, J	0.32	0.18	0.12	0.08
		Disp. mm	2.75	2.00	1.60	1.13
	100 mm/min	%Hyst.	21.4	—	7.8	—
		Energy, J	0.27	—	0.11	—
		Disp. mm	2.55	—	1.50	—
B. POM + 10% TPU	0.3 mm/min	%Hyst.	60.3	49.8	41.9	32
		Energy, J	0.64	0.45	0.24	0.12
		Disp. mm	6.25	4.75	3.20	1.90
	2.0 mm/min	%Hyst.	52.4	41.4	37.0	30.5
		Energy, J	0.58	0.34	0.21	0.12
		Disp. mm	4.60	3.30	2.65	1.78
	20 mm/min	%Hyst.	43.9	—	26.8	—
		Energy, J	0.46	—	0.17	—
		Disp. mm	3.90	—	2.20	—
	100 mm/min	%Hyst.	35.1	—	18.6	—
		Energy, J	0.37	—	0.16	—
		Disp. mm	3.40	—	2.3	—

POM/TPU blend was detected while previous study showed about 2°C increase (15).

Critical Strain Energy Release Rate Gc in Impact

The Gc derived from the basic fracture mechanics in terms of energy absorbed by the conventional Izod impact test has been previously developed (16, 25). The energy absorbed by the impact at fracture rather than at the maximum load is assumed to deform in a totally elastic manner so that the compliance, C, is a function of crack length and the geometry. Thus, for an applied load P resulting in deflection x, we have,

$$x/P = C(a), \text{ a is the crack length} \quad (1)$$

The energy absorbed will be the area under the triangular load-displacement diagram,

$$W = 0.5 Px = 0.5 P^2C \quad (2)$$

For a specimen of uniform thickness B, then the strain energy release rate G is given by,

$$G = (1/B)(dW/da) \quad (3)$$

When G = Gc, a critical value, the elastic and brittle fracture occurs.

$$Gc = (P^2/2B)(dC/da) \quad (4)$$

From Eqs 2 and 4, we obtain the following relation,

$$W = Gc BD\phi \quad (5)$$

and

$$\phi = C/dC/(a/D) \quad (6)$$

If φ is determined as a function of (a/D) and the energy measured is plotted as function of BDO for

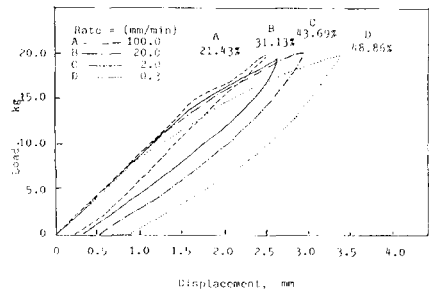


Fig. 17. Effect of deformation rate on hysteresis ratio and deformation strain for POM at 20.0 Kg maximum load.

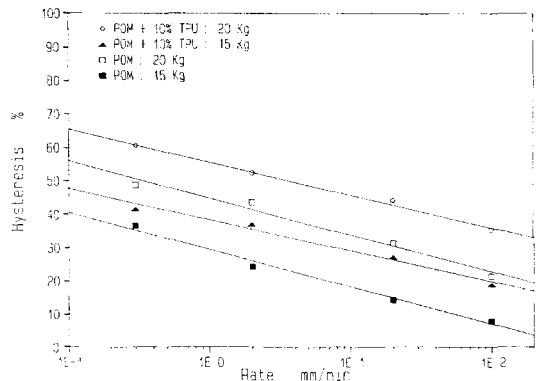


Fig. 18. The relation of deformation rate and hysteresis ratio at maximum loads of 20 and 15 Kg for POM and POM + 10 percent TPU elastomer.

different geometries, a straight line of slope Gc should result. The parameter φ can be determined experimentally by using Eq 6 or through a theoretical calculation. We employed the φ values previously

reported (16) in our study. The plots of impact energy,  $J$ , vs.  $B \cdot D \cdot \phi$  of POM and TPU elastomer modified POM are shown in Fig. 20 and summarized in Table 4. The increase of critical strain energy release rate with the increase of TPU elastomer contents indicates that the TPU elastomer increases the energy dissipation through localized shear yield. The  $G_c$  of the POM + 30 percent TPU is significantly higher than other compositions. Probably due to the greater plastic zone size and other inelastic properties, data from the composition, POM + 30 percent TPU (Fig. 20), do not fit the line well and are thus questionable. However, previous data on tensile properties also showed this

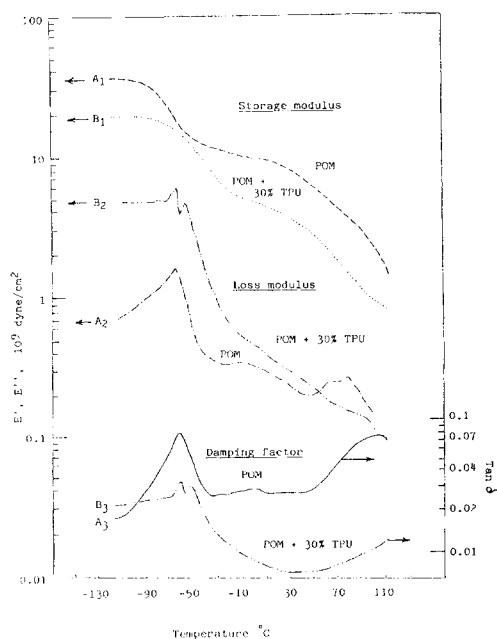


Fig. 19. Storage modulus, loss modulus, and damping factor vs. temperature for POM and POM + 30 percent TPU.

- A<sub>1</sub>: POM, storage modulus,  $E'$
- A<sub>2</sub>: POM, loss modulus,  $E''$
- A<sub>3</sub>: POM, damping factor,  $Tan\delta$
- B<sub>1</sub>: POM + 30% TPU, storage modulus,  $E'$
- B<sub>2</sub>: POM + 30% TPU, loss modulus,  $E''$
- B<sub>3</sub>: POM + 30% TPU, damping factor,  $Tan\delta$ .

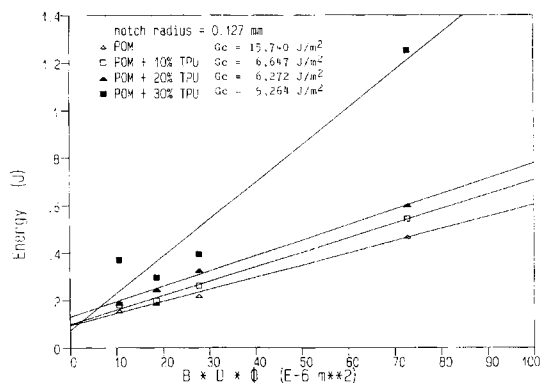
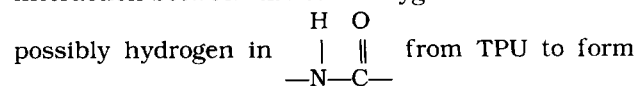


Fig. 20. Critical strain energy release rate ( $G_c$ ) and the plots of  $B \cdot D \cdot \phi$  vs. impact energy for POM and POM + TPU elastomer.

composition has about 6 times greater elongation to break than POM + 20 percent TPU. It appears that significant improvement in POM toughness is achieved by the increase of TPU elastomer content from 20 to 30 percent.

### Fourier Transform Infrared Spectroscopy

FTIR has gradually become a powerful tool to study polyblend miscibility. If the blend is totally immiscible, the absorption spectrum of the blend will be the sum of those for the components. If the blend is miscible or partially miscible, an interaction between the two components perturbs the bonding between atoms; then differences will be noted in the spectrum of the blend relative to the sum of those for the components. Since these changes may be very small, FTIR is usually necessary. The IR investigation of a miscible blend will not only reveal the presence of an interaction, but will provide information on which groups are involved in interaction. Since POM is very difficult to dissolve in solvent for film casting, a multiple internal reflection attachment (ATR) was employed. The FTIR spectra of POM, POM + 20 percent TPU, and TPU are shown in Fig. 21 for comparison. Three major peaks, 1092.8, 926.6, and 895.1  $cm^{-1}$  are in POM and the later two relate to the ether bonding (26). The presence of TPU shifts these two ether peaks to 935.5 and 904.1  $cm^{-1}$  which indicates interaction between the ether oxygen from POM and



hydrogen bonds. The appearance of a weak peak at 1712.8  $cm^{-1}$  (Fig. 21, spectrum B) is indicative of hydrogen bond formation. Partial miscibility of POM and TPU due to hydrogen bond formation is thus assumed.

### CONCLUSIONS

1. POM is a very brittle polymeric material which can be effectively toughened by the introduction of thermoplastic polyurethane elastomer. Toughness improvement on POM is most significant by the increase of TPU content from 20 to 30 percent.
2. POM does fracture in ductile mode under an extremely slow deformation rate of 0.5 mm/min or less and the ductile-brittle transition rate increases with the increase of TPU elastomer content.
3. The hysteresis energy of the precrack specimen is increased with an increase in elastomer content but decreased with an increase in deformation rate. Higher hysteresis energy results in greater precrack plastic zone size and thus tends to shift the fracture mode from brittle to ductile when the critical size of the precrack plastic zone is exceeded.
4. Partial miscibility present between POM and TPU probably due to the hydrogen bond formation that makes TPU elastomer an effective toughening agent for POM.
5. By employing the slow rate fracture method, the advantages of ranking toughness of very brittle ma-

Table 4. Critical Strain Energy Release Rate, Gc.

	Sample			
	POM	POM + 10% TPU	POM + 20% TPU	POM + 30% TPU
a (mm)	0.5	0.5	0.5	0.5
B.D. $\phi$ , m $\times 10^{-6}$	72.78	72.78	72.78	72.78
Energy (J)	0.468	0.545	0.598	1.250
a (mm)	1.47	1.47	1.47	1.47
B.D. $\phi$ , m $\times 10^{-6}$	27.76	27.76	27.76	27.76
Energy (J)	0.225	0.263	0.328	0.398
a (mm)	2.54	2.54	2.54	2.54
B.D. $\phi$ , m $\times 10^{-6}$	18.69	18.69	18.69	18.69
Energy (J)	0.193	0.200	0.250	0.380
a (mm)	3.85	3.85	3.85	3.85
B.D. $\phi$ , m $\times 10^{-6}$	10.61	10.61	10.61	10.61
Energy (J)	0.153	0.178	0.188	0.372
Gc, J/m <sup>2</sup>	5.246	6.272	6.647	15.740

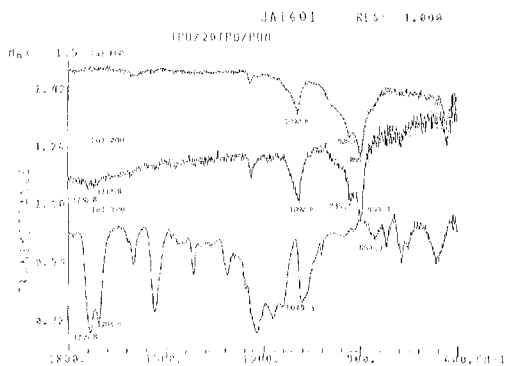


Fig. 21. FTIR-ATR spectra of (a). POM, (b). POM + 20 percent TPU, (c). TPU.

materials can be achieved easier than by varying temperature but maintaining constant impact velocity.

6. Delamination in the buffer region between plane-strain and plane-stress is discovered. The highest strain gradient of the unyielded material immediately outside the yield zone at this buffer region

initiates stress-induced crazes or cavitations as precursor of the observed delamination.

#### ACKNOWLEDGMENTS

The authors wish to thank China Technical Consultants, Inc., Republic of China, for the financial support. Thanks also extend to Prof. Wen-Yen Chiang, Dept. of Chem. Engineering, Tatung Inst. of Technology, for his help in obtaining the dynamic mechanical properties.

#### REFERENCES

1. A. Butlerov, *Ann.*, **111**, 242 (1859).
2. U.S. Patent, 2,768,994 (1956).
3. British Patent, 770,717 (1957).
4. U.S. Patent, 3,027,352.
5. U.S. Patent, 3,795,715.
6. U.S. Patent, 3,850,837.
7. U.S. Patent, 3,476,832.
8. U.S. Patent, 3,642,940.
9. U.S. Patent, 3,749,755.
10. U.S. Patent, 4,277,577.
11. European Patent, 0,116,456,A1.
12. European Patent, 0,117,664,A1.
13. European Patent, 0,120,711,A2.
14. E. A. Flexman, Jr., *Mod. Plast.*, p. 72, Feb. 1985.
15. W. Y. Chiang and M. S. Lo, *J. Appl. Polym. Sci.*, **36**, 1685 (1988).
16. E. Plati and J. G. Williams, *Polym. Eng. Sci.*, **15**, 470 (1975).
17. S. Wu, *Polym. Eng. Sci.*, **27**, 335 (1985).
18. F. C. Chang and L. H. Chu, to be published.
19. E. H. Andrews, *J. Mater. Sci.*, **9**, 887 (1974).
20. E. H. Andrews and E. W. Billington, *J. Mater. Sci.*, **11**, 1354 (1976).
21. E. H. Andrews and Y. Fokahori, *J. Mater. Sci.*, **12**, 1307 (1977).
22. E. H. Andrews, *Makromol. Chem. Suppl.*, **2**, 189 (1979).
23. F. J. Furno, R. S. Webb, and N. P. Cook, *J. Appl. Polym. Sci.*, **8**, 101 (1964).
24. H. R. Brown, *J. Mater. Sci.*, **8**, 941 (1977).
25. G. P. Marshall, J. G. Williams, and C. E. Turner, *J. Mater. Sci.*, **8**, 949 (1973).
26. G. V. Schulz, *Makromol. Chem.*, **186**, 2061 (1985).